Modeling Water Table Trends in High-Latitude Peatlands: Divergent Hydrological Responses and Fire Risk Implications

Piotr Janiec[1,2], Mariusz Lamentowicz[3], Katarzyna Marcisz[3], Hui Zhang[4], Minna Väliranta[5], Jakub Nowosad[1, 6]

[1] Department of Geoinformation, Adam Mickiewicz University, Poznań, Poland

[2] *Department of Forest Resources Management, Faculty of Forestry, University of Agriculture, Kraków, Poland*

[3] Climate Change Ecology Research Unit, Adam Mickiewicz University, Poznań, Poland

[4] State Key Laboratory of Lithospheric and Environmental Coevolution, Institute of Geology and Geophysics, Chinese Academy of Sciences, Beijing, China

[5] Environmental Change Research Unit (ECRU), Ecosystems and Environment Research Programme, University of Helsinki, Helsinki, Finland

[6] Institute of Landscape Ecology, University of Münster

Corresponding author: Piotr Janiec

Key words: permafrost, Northern Hemisphere, hydrology, carbon, peatland, climate change, modeling, area of applicability.

Abstract

Permafrost peatlands are especially important in the Northern Hemisphere, where global warming is observed at much faster rates than at lower latitudes. Yet, large-scale assessment of permafrost peatland water table trends has not been conducted. Here, we modeled 103 peat records from high-latitude peatlands, calibrating against 53 explanatory variables that describe regional environmental conditions. We tested multiple modeling approaches and identified the area of applicability of the derived model. The random forest model achieved the best performance (RMSE = 0.48, MAE = 0.38). Our results reveal divergent peatland responses to global warming, with elevation, precipitation seasonality, and climate moisture index emerging as the most influential drivers. We further demonstrate that water table depth significantly influences wildfire occurrence, with marked differences in fire frequency between regions showing drying versus wetting trends. This study highlights key knowledge gaps in palaeoenvironmental high-latitude peatland research and underscores the need for intensified global modeling of peatland hydrological conditions.

Introduction

Progressing global warming influences ecosystems worldwide, and the effect of this pressure are increasingly well predicted by models (Pörtner et al., 2022). Increasing annual temperatures, heat waves, seasonal changes in rainfall patterns, and more frequent catastrophic events such as tornadoes, fires or floods are becoming more intense in many areas of the

Earth (Lee et al., 2023). Environmental pressure is modifying various ecosystems, and the acceleration of these changes is especially visible in high latitudes through shrubification of the Arctic and northern peatlands (Buchwal et al., 2020; Buttler et al., 2023). Comparing ongoing climate changes with past geological periods, there is a high probability that high-latitude regions will be affected mainly through progressing global warming (Fischer et al., 2018).

Peatlands are sensitive ecosystems responding to the impacts of changing climate and human activity. Many studies conducted in the past years have documented, through observation , monitoring and palaeoecology, significant disturbances of peatland functioning (e.g. permafrost thawing, more frequent droughts and fires) (Artz et al., 2022; Burdun, Bechtold, Sagris, Komisarenko, et al., 2020; Gałka et al., 2022; Heinemeyer & Swindles, 2018; Lamentowicz et al., 2019; Magnan et al., 2019; Marcisz et al., 2023; Słowińska et al., 2022; Zhang et al., 2022). Such observations underlined that disturbances connected with human impact and climate change negatively influence peatlands. Whether due to climate (Bragazza, 2008; Loisel et al., 2021) or anthropogenic (Tanneberger et al., 2021), the effect has been substantial water table lowering observed in peatlands over the last several hundred years (Swindles et al., 2019). Lower water tables lead to exposure of surface peat layers to fires (Kettridge et al., 2015; Turetsky et al., 2015) or even zombie fires observed in northern peatlands (Witze, 2020). All these processes lead to a loss of peat carbon and carbon emissions to the atmosphere, strengthening climate warming (Harenda et al., 2018). Peatlands are a critical component in atmospheric carbon sequestration (Gallego-Sala et al., 2018; Karpińska-Kołaczek et al., 2024; Turetsky et al., 2015). Yet, because it is challenging to model peatland functioning, including water table changes and carbon dynamics (Blodau, 2002; Zhang et al., 2022), peatlands are not included in most of the Earth System Models for the Coupled Model Intercomparison Project Phase 6 (Canadell et al., 2021). The difficulty arises from the strong spatial heterogeneity of peatlands, complex feedback mechanisms between hydrology and carbon cycling, and limited long-term datasets for model calibration and validation. Although recent advances such as ORCHIDEE-PEAT (Qiu et al., 2019) and the JULES peatland scheme (Chadburn et al., 2022) demonstrate progress toward explicitly representing peatland processes, substantial challenges remain in capturing their dynamic feedbacks under climate change. As peatland hydrology and carbon sequestration are tightly interconnected, improving their representation in Earth System Models is essential for more accurate estimates of their role in the global carbon balance.

Large-scale spatial monitoring and modeling using remote sensing data have become increasingly popular in environmental research due to advancements in satellite technology and data processing. Remote sensing provides a valuable tool for capturing vast areas over long periods, enabling the monitoring of ecosystems at a large scale with unprecedented precision. Traditional methods for large-scale mapping, such as the manual digitization of aerial photographs (Cruickshank & Tomlinson, 1990; Vitt et al., 2000), were labor-intensive, time-consuming, and costly to implement. These approaches were limited in scope and primarily focused on visible environmental changes rather than the underlying processes causing those changes. As the demand for more efficient and scalable monitoring techniques grew, modern methods have been developed that leverage time series data from satellites, offering a more compre-

hensive and automated approach. Satellite-based monitoring allows for the continuous tracking of environmental changes across extensive regions, especially in remote and difficult-to-access areas like peatlands.

Recently, new techniques have been developed to monitor the conditions of peatlands over extended periods using satellite time series data. These methods allow for detecting subtle environmental shifts that may not be immediately visible through traditional observations. However, despite the advancements in remote sensing technology, most current peatland monitoring still relies on data derived from optical or microwave sensors, thus only utilizing a fraction of the available spatial information (Asmuß et al., 2019; Bechtold et al., 2020; Burdun, et al., 2020a; Burdun, et al., 2020b; Räsänen et al., 2022).

In-situ observations and remote sensing data are often used to model various environmental properties and processes. Statistical modelling, especially machine learning methods, allows for selecting explanatory variables and non-linear model building. Most studies use linear regression or random forest, and the explanatory variables are based on optical or radar remote sensing (Bechtold et al., 2018; Bourgeau-Chavez et al., 2005; Kim et al., 2017; Klinke et al., 2018; Millard & Richardson, 2018; Räsänen et al., 2022a; Torbick et al., 2012). In a recent study, Huang et al. (2021) used random forest method (RF) and multiple explanatory variables to assess the tradeoff between carbon dioxide and methane emissions from global peatlands. Pang et al. (2023) used the RF method for the upscaling field measurements in the peatlands. To our knowledge, global-scale modeling of peatland water table depth (WTD) trends has not yet been conducted. Previous studies have applied similar approaches at regional scales, such as in the Flow Country bogs of Scotland (Toca et al., 2020) and across Finland (Räsänen et al., 2022b), providing valuable foundations. However, our study is the first to extend such modeling to high-latitude peatlands at the global scale, enabling the assessment of large-scale patterns and drivers of WTD change. The availability of ground truth, climate, topography and land cover products opens new possibilities for using an indirect approach and modelling the WTD on a large scale (Olefeldt et al., 2021). Integrating multiple spatial data types makes it feasible to create entirely novel models (Olefeldt et al., 2021). Using wildfires as an example here, we demonstrate how valuable a product can be in assessing WTD trends. Understanding this relationship is crucial, as WTD is a key factor in regulating soil moisture and, consequently, the availability of combustible material (Turetsky et al., 2015). Previous research has shown that lower WTD levels, often associated with climate-induced drying trends, can increase the vulnerability of peatlands to fire, leading to more intense and widespread burn events (Van Der Werf et al., 2017). Since Arctic wetlands are significant carbon sinks (Hugelius et al., 2020), fires exacerbated by WTD fluctuations could contribute to increased carbon emissions and further climate feedback loops (Kettridge et al., 2015). Therefore, investigating this relationship is essential for predicting future fire regimes in the Arctic and developing strategies for ecosystem conservation and climate mitigation.

The primary purpose of this study is to model the WTD trends in the high-altitude peatlands of the Northern Hemisphere using remote sensing data. We used peatland palaeohydrological records and various explanatory variables to calibrate the model, which describe the region's environmental conditions. Our specific objectives were to: (a) find the most critical variables

that influence the WTD in the area of interest; (b) model the WTD trends in the study area; (c) find the area of applicability of the derived model. A secondary goal of our study was to determine whether WTD fluctuations influence the scale of fire occurrences in the study area.

Materials

Peat records

We used 103 peat records previously compiled and published by Zhang et al. (2022). In that study, the authors derived the hydrological proxy used here by reconstructing water-table depth (WTD) from peat-core testate amoeba assemblages using established modern training sets and transfer functions. For each record, sample ages were assigned using Bayesian age-depth models based on available chronological controls (e.g., radiocarbon, ^210Pb, and other stratigraphic markers), and taxa were harmonised to ensure compatibility with the training sets. WTD was then reconstructed using the most appropriate regional/Holarctic transfer function for each site. For a detailed description of the reconstruction process and hydrological response analysis, see Zhang et al. (2022).

From this dataset, we selected sites located in the permafrost areas only and filtered the WTD values for the years 2001-2018 (Fig. 1). The selection of these years was based on the availability of the MODIS satellite data for the specified period. Consequently, we generated a dataset comprising 181 annual WTD values from 52 sites within permafrost regions. Zhang et al. (2022) provide standardized (unitless) WTD reconstructions; therefore, our continuous models predict standardized WTD. The standardized values of WTD ranged from -3.00 to 3.60 with a mean of 0 and standard deviation of 0.97. We also performed a non-parametric Mann-Kendall trend test (Hamed & Rao, 1998) to characterize both positive and negative trends of the WTD in the analyzed period, using the Kendall package (McLeod, 2005) in the R environment (R Development Core Team, 2023). We have divided the TAU values into two categories: those with drying trends and those with wetting trends.

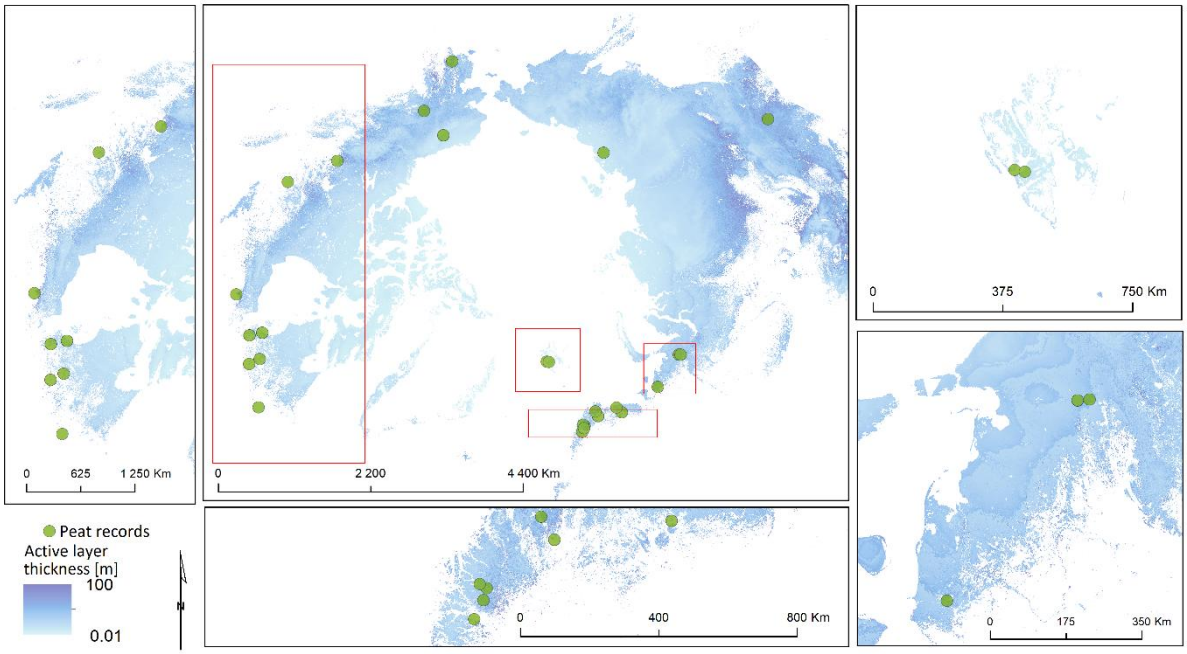

Fig. 1. Location of the study area and peat records analysed in the permafrost region of the northern hemisphere.

Explanatory variables

Based on the previously published data (Belyea & Baird, 2006; Gallego-Sala et al., 2018; Li et al., 2023; Loisel et al., 2012, 2021; Rydin et al., 2013)(Table 1), we selected to test 53 explanatory variables. The variables were divided into six categories: meteorological, bioclimatic, vegetation, permafrost, topography, and latitude.

Table 1. The explanatory variables employed in the study were categorised into six distinct groups: meteorological (blue), bioclimatic (yellow), vegetation (green), permafrost (grey), topography (black) and latitude (orange).

Variable	Full name	Temporal resolution [years]	Lag	Spatial resolution [m]	Source
clt	cloud area fraction	1	Yes	1000	CHELSA-W5E5 v1.0: W5E5 v1.0 downscaled with CHELSA v2.0
cmi	climate moisture index				
hurs	near-surface relative humidity				
pet	potential evapotranspiration				
pr	precipitation amount				
rsds	surface downwelling shortwave flux in air				
sfcWind	near-surface wind speed				
tas	mean daily air temperature				
tasmax	mean daily maximum 2 m air temperature				

tasmin	mean daily minimum air temperature				
vpd	vapor pressure deficit				
bio1	annual mean temperature	-	No	1000	WorldClim 1
bio2	mean diurnal range (mean of monthly (max temp - min temp))				
bio3	isothermality (bio2/bio7) (×100)				
bio4	temperature seasonality (standard deviation ×100)				
bio5	max temperature of warmest month				
bio6	min temperature of coldest month				
bio7	temperature annual range (bio5-bio6)				
bio8	mean temperature of wettest quarter				
bio9	mean temperature of driest quarter				
bio10	mean temperature of warmest quarter				
bio11	mean temperature of coldest quarter				
bio12	annual precipitation				
bio13	precipitation of wettest month				
bio14	precipitation of driest month				
bio15	precipitation seasonality (coefficient of variation)				
bio16	precipitation of wettest quarter				
bio17	precipitation of driest quarter				
bio18	precipitation of warmest quarter				
bio19	precipitation of coldest quarter				
EVI	enhanced vegetation index	1	Yes	250	MODIS/006/MOD13Q1
NDVI	normalized differenced vegetation index				
Greenup_1	date when EVI first crossed 15% of the segment EVI amplitude	1	Yes	500	MCD12Q2
MidGreenup_1	date when EVI first crossed 50% of the segment EVI amplitude				

Peak_1	date when EVI reached the segment maximum				
Maturity_1	date when EVI2 first crossed 90% of the segment EVI amplitude				
MidGreendown_1	date when EVI last crossed 50% of the segment EVI amplitude				
Senescense_1	date when EVI last crossed 90% of the segment EVI amplitude				
Dormancy_1	Date when EVI last crossed 15% of the segment EVI amplitude				
EVI_Minimum_1	segment minimum EVI value				
EVI_Amplitude_1	segment maximum - minimum EVI				
EVI_Area_1	sum of daily interpolated EVI from Greenup to Dormancy				
ALT	permafrost active layer thickness	1	Yes	1000	ESA Permafrost Climate Change Initiative (Permafrost_cci): Permafrost active layer thickness for the Northern Hemisphere, v3.0
GST	ground permafrost surface temperature				Permafrost ground temperature for the Northern Hemisphere, v3.0 from MODIS LST, ERA5, 1997-2019
T1m	ground temperature 1 m				
T2m	ground temperature 2 m				
T5m	ground temperature 5 m				
T10m	ground temperature 10 m				
DEM	elevation	-	No	90	MERIT DEM: Multi-Error-Removed Improved-Terrain DEM
slope	sine slope				
aspect_cos	cosine aspect				
aspect_sin	sine aspect				
latitude	Y	-	No	-	-

The meteorological variables were derived from the CHELSA data set (Brun et al., 2022). The data had 30 arc sec (~1 km) spatial resolution. We calculated the annual mean values of the 11 variables from the monthly rasters. We also used 19 bioclimatic variables from the WorldClim data set (Hijmans et al., 2005) with the spatial resolution of 30 arc sec (~1 km). In order to generate more biologically meaningful variables, the monthly temperature and rainfall values were used as the basis for the derivation of bioclimatic variables. To ensure the reliability of the analysis, bioclimatic and meteorological variables from various sources were employed

to account for the discrepancies in the methodologies utilized in the generation of the two data sets. This approach was undertaken to prevent the analysis from being unduly influenced by the inherent limitations of the data sources.

To assess the influence of vegetation on the WTD, we employed the use of the Normalized Difference Vegetation Index (NDVI) and the Enhanced Vegetation Index (EVI) from the MODIS/006/MOD13Q1 product, which has a spatial resolution of 250 meters and a temporal resolution of 16 days. The mean annual values were calculated for each of the indexes. Besides this, we used 10 global land cover dynamics variables derived from the MCD12Q2 product with the 500 meters' spatial resolution and annual temporal resolution. These products are based on the MODIS (Terra Moderate Resolution Imaging Spectroradiometer) (Savtchenko et al., 2004). The data were processed in the Google Earth Engine (GEE) (Gorelick et al., 2017).

The six topography variables were calculated from the MERIT DEM (Multi-Error-Removed Improved-Terrain Digital Elevation Model). The MERIT DEM is a high-accuracy global DEM at 3 arc second resolution (~90 m) produced by eliminating major error components from existing DEMs (Digital Elevation Models) (NASA SRTM3 DEM, JAXA AW3D DEM, Viewfinder Panoramas DEM) (Yamazaki et al., 2017). For the aspect calculation, we used cosine-sine encoding (Stage, 1976), a commonly used approach for preprocessing cyclical variables in machine learning models to avoid misinterpreting by the algorithms (Brenning et al., 2015; Stage & Salas, 2007). We also included latitude in the model to incorporate the geographical location of the sample plots. This approach has been tested in multiple studies and has improved the model accuracy (Andersen et al., 2022; Lyons & Willig, 2002; Zintzen et al., 2017).

Fire data

To assess the impact of WTD trends on wildfire occurrence, we utilized data from the Fire Information for Resource Management System (FIRMS) archive (Davies et al., 2008). FIRMS provides near real-time fire detection data from NASA's satellite-based sensors, including the Moderate Resolution Imaging Spectroradiometer (MODIS) and the Visible Infrared Imaging Radiometer Suite (VIIRS). For this study, we selected MODIS fire data for its longer temporal record, allowing for a more extended historical analysis of wildfire patterns. We used the data recorded between 2001 – 2018. MODIS, aboard the Terra and Aqua satellites, provides global fire observations at a spatial resolution of 1000 m and a temporal resolution of four daily observations per location. For the analysis we filtered only records with a confidence higher than 50 %.

Methods

Overall workflow of the WTD modelling

The proposed methodology is based on the processing of explanatory variables and their modelling for the purpose of developing a WTD changes model (Fig. 2).

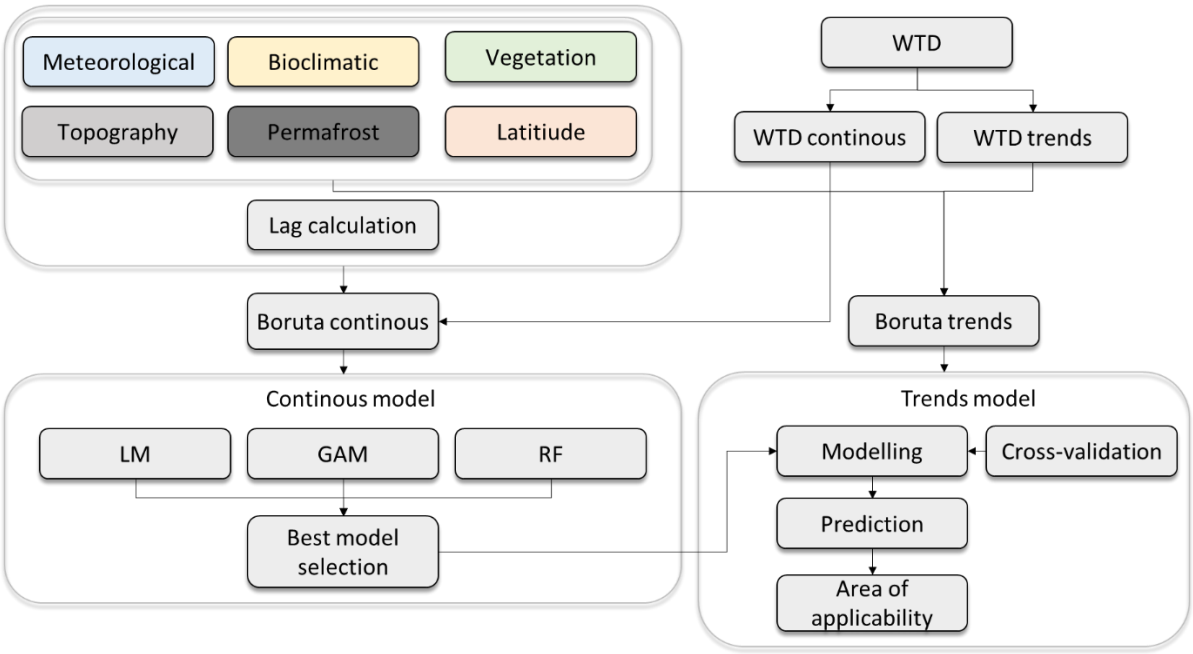

Fig. 2. General workflow of the WTD modelling.

Preprocessing

Ecological systems often exhibit temporally lagged responses to environmental changes (Lira et al., 2019). To account for this temporal lag, we generated two versions of each time-varying predictor: a contemporaneous (*year t*) dataset and a one-year lagged (*year t-1*) dataset. All subsequent analyses were performed in parallel using both predictor sets to evaluate whether lagged conditions improved the prediction of WTD. We resampled the variables to a spatial resolution of 1000 meters and ensured all data were aligned within the same coordinate system (WGS 1984). The resampling was performed by adjusting the data grid to match the desired resolution using the bilinear interpolation method. In the subsequent phase of the analysis, the pixel values were extracted from each variable within the designated area of each sample plot. Thereafter, the mean values of the variables were calculated for each WTD value and WTD trend.

Variable importance

We used the Boruta algorithm implemented in the "Boruta" R package (Kursa & Rudnicki, 2010) to compare the importance of each variable to randomly permuted variables and find the significant ones. Boruta is based on the RF classifier. The algorithm duplicates the variables and shuffles them to remove correlations with the response. In the next step, Z-scores are computed during the random forest computations. Then, the algorithm checks if the real variables have higher Z-scores than the maximum Z-score of shadow variables. The Z-score measures how many standard deviations below or above the population mean a raw score is. The variables which have Z-score significantly lower importance than shadow variables are "unimportant". The variables that have a Z-score significantly higher importance than shadow variables are marked as "important" (Kursa & Rudnicki, 2010). We applied the Boruta algorithm for two scenarios: WTD continuous values and WTD trends.

Models

We tested three techniques for WTD continuous values modeling: multiple linear regression (MLR), generalized additive models (GAM), and random forest (RF). Each technique was tested using only important variables selected by the Boruta algorithm.

An MLR is an extension of the simple linear regression model for data with multiple predictor variables and one response variable. It models the linear relationship between the predictor and response variable (Eberly, 2007). The MLR formula is as follows (Eberly, 2007):

$$y_i = \beta_0 + \beta_1 x_{i1} + \beta_2 x_{i2} + \cdots + \beta_{p-1} x_{i,p-1} + \varepsilon_i$$

where, for i = n observations, refers to the intercept and β_p are slope coefficients for each explanatory variable. ε_i is a model's error term, also known as the residuals. The MLR algorithm is commonly used for modeling spatial ecological data due to its simplicity of calculation and interpretation (Beale et al., 2010; Knoll et al., 2019; Xie et al., 2021). The main disadvantage of the MLR is that we cannot observe the nonlinear relationships between the predictors and response variables (Zhang et al., 2017).

To include the nonlinear relationships in the model we used GAM, which is a semiparametric extension of generalized linear models (GLM) (Guisan et al., 2002; Hastie, 1992). The general form of the GAM model is described by the equation:

$$g(\mu_i) = x_i \alpha + \sum_{j=1}^{m} f_j(x_i, \mathrm{j})$$

where $\mu_i = E(y_i)$, y_i is the response variable, $E(.)$ denotes the expected value of a random variable, x_i is the i-th row of the model matrix for the parametric model components, and f_j is a smoothing function of x_j (Hastie, 1992). GAM models are widely used in ecological modeling due to their high flexibility and easy interpretation (Leathwick et al., 2006).

The RF algorithm is relatively quick and can usually be run without tuning parameters in the comparison with other machine learning algorithms. RF is an extension of CART (classification and regression trees) developed by Breiman (2001). RF is defined as a collection of tree-structured weak learners comprised of identically distributed random vectors where each tree contributes to a prediction for *x*. Ensemble-based weak learning hinges on diversity and minimal correlation between learners. RF introduces diversity by using bootstrap sampling of the training data and, at each split in a tree, randomly selecting a subset of predictor variables from the full set of variables (Breiman, 2001; Evans et al., 2011).

Validation and best model selection

The main objective of the study was to identify the variables and algorithms capable of explaining the change in WTD levels in permafrost peatlands. As we had a very limited number of observations (181) for a very diverse area and a large aerial extent, we decided not to split the data on the training and validation datasets during the best model selection phase (continuous WTD values). To assess the WTD error in the models we calculated mean absolute error (MAE) and RMSE (root mean squared error) based on the equations:

$$RMSE(y, \hat{y}) = \sqrt{\frac{\sum_{i=0}^{N-1}(y_i - \hat{y}_i)^2}{N}}$$

where, y_i is the measured value; $\hat{y}_i$ is the predicted value; i is the summation index; N is the number of cases. We also calculated bias as the average amount by which the actual value is greater than the predicted value.

After the best model selection for the continuous WTD data, we tested the categorical model (drying or wetting trends), with best performing algorithm. We used the 10-fold cross-validation for the model validation. We have calculated Cohen's kappa coefficient (K) and Overall Accuracy (OA) based on the confusion matrix (Cohen, 1960):

$$K = \frac{OA - EA}{1 - EA}$$

where, the overall accuracy (OA) was calculated by dividing the sum of all true positive (TP) and true negative (TN) classification results by the total amount of data.

Prediction and area of applicability

The objective was to predict the spatial WTD trends over the past 20 years, with the aim of identifying the most appropriate model for this purpose. The northern circumpolar permafrost zone was selected as the area of interest based on the Arctic Circumpolar Distribution and Soil Carbon of Thermokarst Landscapes map (Olefeldt et al., 2016). Given the limited training data available for the model, we sought to evaluate its area of applicability (AoA) (Meyer & Pebesma, 2021). Based on the available training data, the AoA refers to the spatial extent under which a model's predictions or outputs are reliable and valid. For this purpose, we employed the AOA function from the CAST R package (Meyer et al., 2025). The function estimates the Dissimilarity Index (DI) and the derived AOA of spatial prediction models by considering the distance of new data in the predictor variable space to the data used for model training. The AOA is derived by applying a threshold on the DI which is the (outlier-removed) maximum DI of the cross-validated training data (Meyer & Pebesma, 2021). We created a WTD trends map based on predictions and AOA results in areas where our model is applicable.

Impact of the WTD trends on fire occurrence

We applied the Chi-Square test for independence to determine whether the distribution of wildfire occurrences significantly differed across areas with different WTD trends (McHugh, 2013). The calculations were performed using the *chisq.test()* function in the R environment. This statistical test evaluates whether there is a significant difference between wildfire occurrence and WTD trends across four categorical groups: (1) areas with wetting trends and fire occurrence, (2) areas with drying trends and fire occurrence, (3) areas with wetting trends and no fire occurrence, and (4) areas with drying trends and no fire occurrence. The analysis was conducted only for areas where our model was applicable, as determined by the AOA criteria.

Results

Variable importance

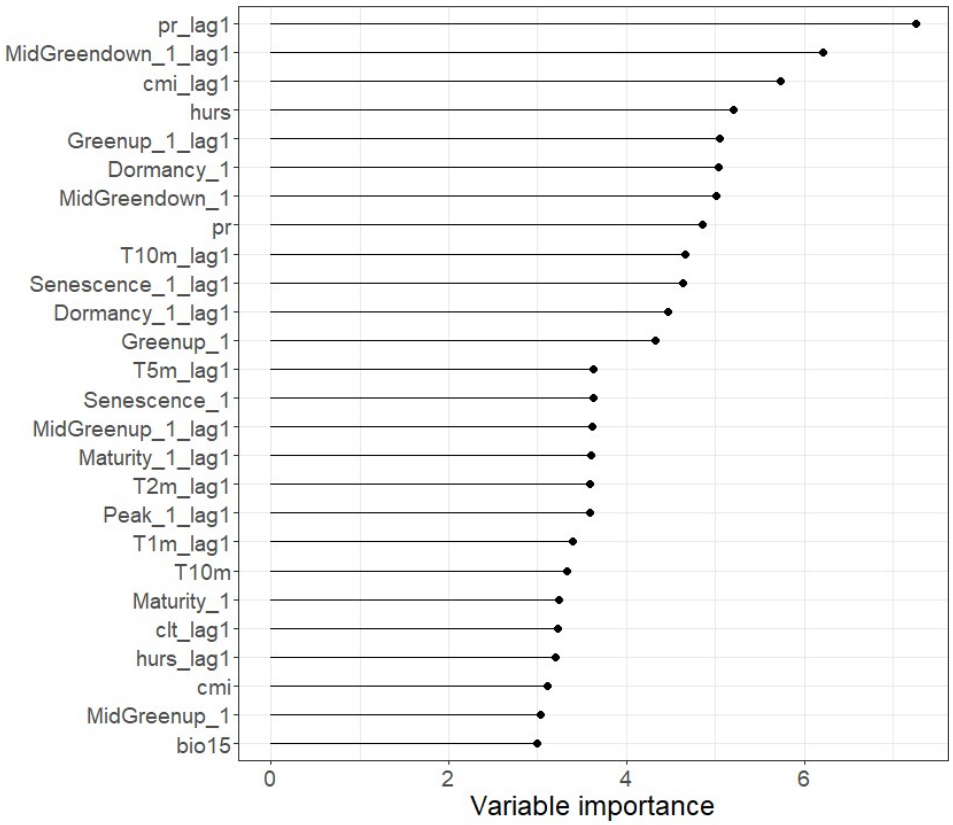

Fig. 3. Variable importance for the continuous WTD model of the variables selected by the Boruta algorithm. Variable codes are described in Table 1.

Of the 83 variables, 26 were of high importance for the WTD (Fig. 3). Lagged variables were more significant than non-lagged variables. The precipitation with a one-year lag (pr_lag1) was the most significant. All significant meteorological variables were related to humidity conditions. Bio15 was the only significant bioclimatic variable. The derivative layers of the EVI and NDVI indices were also found to be of significant importance, and the variables related to the duration of the growing season were particularly important. Permafrost-related variables were also significant. It is notable that the ground temperature at specific altitudes exhibits a considerable degree of variation. However, this phenomenon is only discernible when a one-

year lag is applied. The variables pertaining to topography and latitude were found to be insignificant.

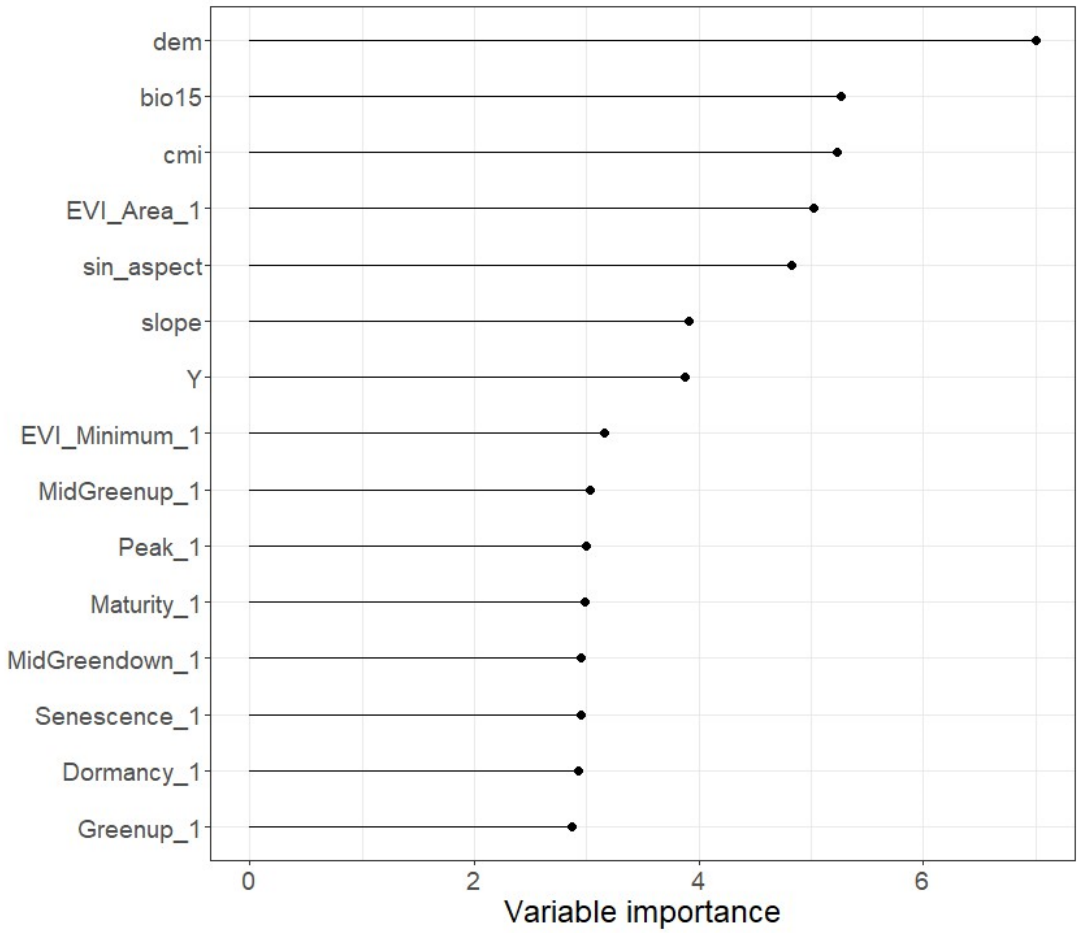

Fig. 4. Variable importance for the WTD trend model based on the variables selected by the Boruta algorithm. Variable codes are described in Table 1.

The variables used to assess WTD trends differed from those used to assess continuous WTD (Fig. 4), where 15 variables were found to be significant. The most significant variable was the DEM, contrary to the continuous WTD values model, where the DEM was found to be insignificant. Of the bioclimatic variables, only bio15 was found to be significant. The CMI was found to be a significant factor concerning the meteorological variables. The principal variables associated with vegetation were those pertaining to the duration of the growing season, as exemplified by the continuous WTD model. In contrast with the variables that are pertinent to the evaluation of the continuous WTD value, the permafrost-related variables are not applicable to the assessment of its trends. However, three topographical variables were important in the model (dem, sin_aspect, slope). Moreover, latitude was important in contrast to the continuous WTD model.

Models and validation

Based on the selected variables, we developed three continuous models for the WTD modelling, each with a different level of accuracy (Table 2).

Table 2. The accuracy of the models tested for the standarized continuous WTD prediction.

model	bias	RMSE	MAE
RF	0.001385	0.48	0.38
LM	6.86E-13	0.75	0.61
GAM	-0.08362	1.10	0.88

The RF model characterized the smallest RMSE (0.48) and MAE (0.38). The GAM model had the highest RMSE (1.10) and MAE (0.88). The bias values closest to 0 were characterized by the LM model, although the other models were also characterized by bias only slightly deviating from 0. Based on the validation results, we selected the RF model for further analysis.

In the next stage, we built categorical (trend) models on each peat record. We have tuned the RF algorithm using variables from the Boruta algorithm that were calculated for trend values. The model was characterized by OA = 0.75 and K = 0.43. The best accuracy was obtained by the model with five predictors: cmi, dem, EVI_Area_1, bio15 and sin_aspect (Fig. 6).

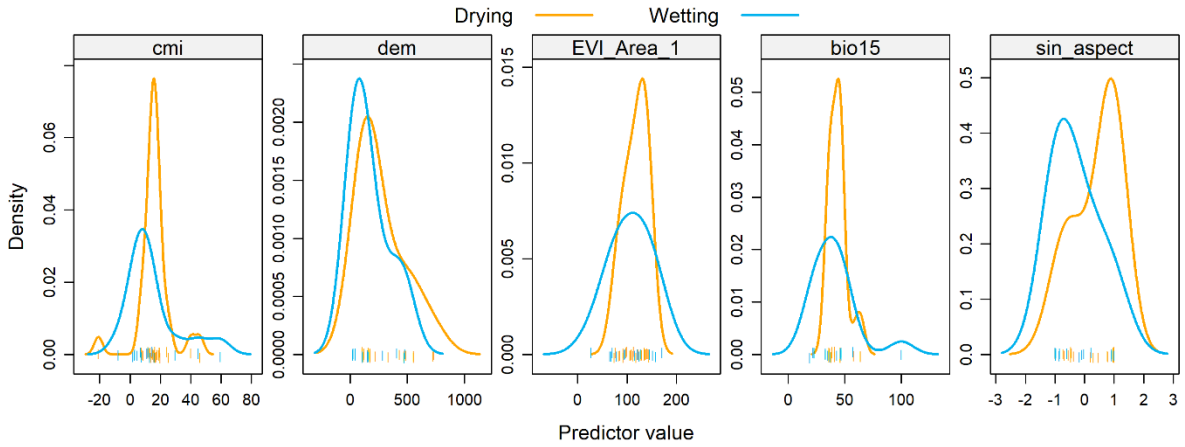

Fig. 6. Density distributions of the highest importance predictors in the categorical WTD trend model (Drying vs Wetting). Lines representdistributions of predictor values for each class.

The drying WTD trend peaks at moderate to high CMI, higher elevations, moderate EVI, and moderate bio15, while the wetting trend was more spread out at lower CMI, lower elevations, lower EVI, and higher bio15. Additionally, the rising WTD trend was linked to negative sin_aspect values, whereas the drying trend was centered around zero.

Prediction and area of applicability

Table 3. The areas of the WTD trends and its area of applicability.

WTD trends	Area [km^2]	% of total area	% within applicable areas
Drying	3330902	22.16	54.43
Wetting	2788547	18.55	45.57
Non-aplicable	8914977	59.3	-

The results indicate that our model is applicable to 40.71% of the study area. Specifically, 18.55% of the area exhibits wetting trends, while 22.16% shows a drying trend. However within applicable areas 54.43% of the areas exhibits drying trends and 45.57% of the areas exhibits wetting trends. The remaining 59.29% of the area did not demonstrate model applicability (Table 3).

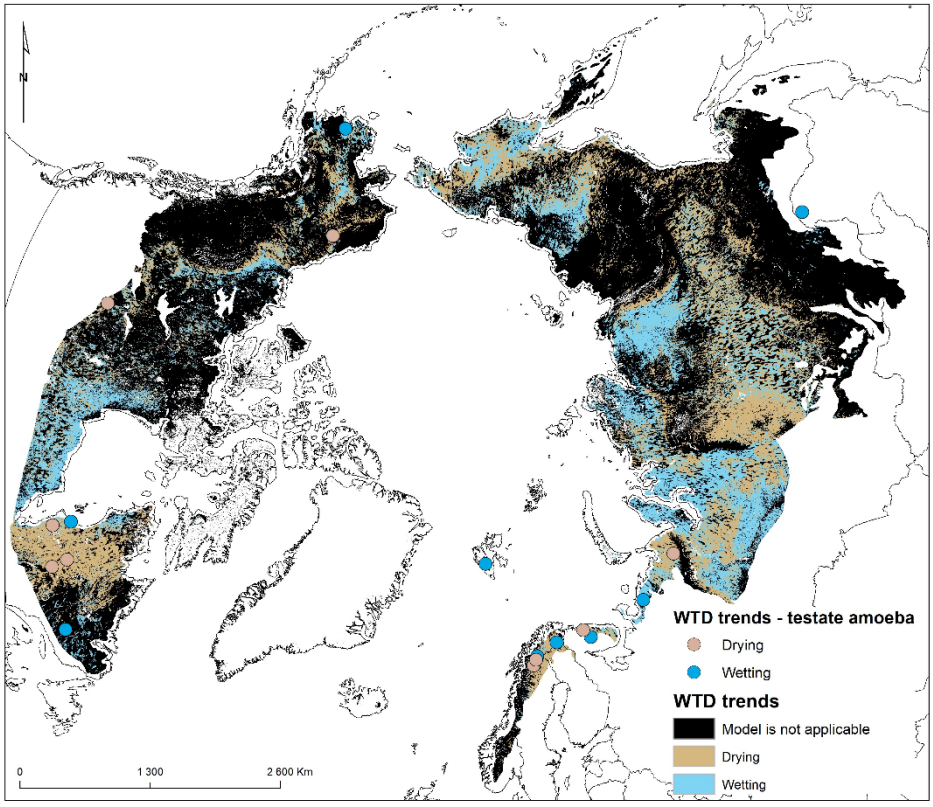

Fig 7. WTD trends model prediction results and area of applicability of the model.

In the Canadian Arctic, where the model is applicable, WTD exhibited drying trends in Eastern Canada over the past 20 years, while central Canada showed wetting trends (Fig. 7). In the European Arctic, WTD generally declined, whereas the Russian Arctic displayed mixed trends, particularly in the Ural region. Southern Siberia experienced drying trends, in contrast to the Far East, where western Yakutia showed wetting trends and the Kolyma region exhibited mixed patterns. The model could not be applied to most of Alaska and to Northern and Eastern Canada based on the area of applicability analysis. Similarly, it was not applicable in central Yakutia or in mountainous regions of the Russian Arctic, notably the Sayan and Yablonovy ranges, as well as parts of the northwestern European Arctic.

Impact of the WTD trends on fire occurrence

Through the development of the WTD map for the study area, we were able to assess whether fires occurring in recent years were related to WTD fluctuations. We also observed a substantial difference between burned areas with drying and wetting trends (Table 4).

Table 4. WTD trends and fire occurrence distribution.

WTD trends	Fire occurence	Area [km^2]	Area percentage
Drying	No fire	3077564	50.29

	Fire	253337	4.14
Wetting	No fire	2613438	42.71
	Fire	175108	2.86

The results revealed a significant difference in fire incidence between areas with drying and wetting trends (Chi-Square test, $p < 2.2e-16$). Most areas experiencing drying trends did not have burning events, accounting for 50.29% of the total area, while only 4.14% of the drying-trend area was affected by fire. For wetting trends, 42.71% of the area showed no burning events, whereas 2.86% experienced fire. When comparing across trends, the proportion of fire-affected areas was slightly higher under drying trends (7.6%) than under wetting trends (6.3%), suggesting that fires occur more frequently in drying regions.

Discussion

Modeling of long-term water table changes

We tested one linear modeling method (MLR) and two non-linear methods (GAM and RF) for predicting WTD. The non-linear models produced the most accurate results, aligning with findings from other studies (Toca et al., 2020). Among these, the RF model demonstrated the highest accuracy. To enhance model efficiency and interpretability, we significantly simplified the model by reducing the number of predictor variables using the Boruta feature selection algorithm. While our large-scale approach is valuable for generating broader generalizations, it inevitably overlooks fine-scale ecological and hydrological processes, potentially obscuring important dynamics. This limitation is particularly relevant in the context of incorporating complex feedback mechanisms into Earth System Models. Our work contributes to this effort by enhancing model efficiency and interpretability: we reduced the number of predictor variables using the Boruta feature selection algorithm, retaining only those most relevant for prediction. This step improves computational efficiency without sacrificing predictive power and is especially important for large-scale or global models, where minimizing input variables reduces data pre-processing time and accelerates predictions while maintaining robustness. Striking a balance between accuracy, simplicity, interpretability, and practical applicability is therefore essential. Future improvements should focus on integrating finer-scale ecological and hydrological processes into ESMs while leveraging efficient feature selection to ensure models remain tractable at global scales (Austin, 2007).

Bechtold et al. (2014) emphasize the need for robust remote sensing-based predictors to explain WTD variability. Combining proxy-based local water table, meteorological, remote sensing and topographical data, we obtained a synthetic look at the causes of the recent hydrology of the high-latitude peatlands. Variables that best explain the water table trend mainly relate to the balance in different biogeographic settings. Interestingly, when modelling WTD annual WTD values, the most important were lagged variables. This suggests that past hydrological conditions, rather than just the current state of the WTD, significantly increase fire risk (Benscoter & Wieder, 2003; Blodau, 2002; Tuittila et al., 2007; Zoltai et al., 1998). Lagged variables represent the delayed effects of prior wet or dry conditions on the ecosystem, particularly in peatland environments where the water table responds slowly to seasonal and interannual fluctuations. When modelling the WTD trends CMI was the most critical factor. CMI is

an indicator of drought calculated as the difference between annual precipitation and potential evapotranspiration; it represents the potential water loss (through evaporation) from a landscape covered by vegetation. This variable related to water availability might be interpreted as the primary driver of peatland wetness and growth (Baird et al., 2009), while it is affected by global warming extremes like progressing heat waves, wetting the water table deficit (Gallego-Sala et al., 2018). CMI (climate moisture index) reflects the consequences of the wetting temperature and higher evapotranspiration that leads to more intensive water loss from peatlands; however, in permafrost areas, it conversely leads to accelerated thawing (Beer et al., 2023; Natali et al., 2021; Piilo et al., 2023; Schuur et al., 2022; Turetsky et al., 2020). Especially in continental regions like Western Siberia, CMI represents the negative water table trends leading to higher carbon emissions and peat fires (Gibson et al., 2018). This variable might predict the occurrence of peat fires (including zombie fires). CMI, in reality, best reflects the recent global climatic trends that are well visible in the peatland vegetation state reflected by the enhanced vegetation index EVI_AREA_1, which is related to the greenness reflecting the vegetation state/health and land cover changes. CMI is correlated with the water availability for peatland plants (Burdun et al., 2023; Connolly et al., 2011; Lees et al., 2020; Schubert et al., 2010; Setiawan et al., 2017). Another variable related to water table position was bio 15 (the Seasonality (standard deviation *100) of Precipitation); different distributions of the precipitation throughout the year might lead to deeper water table deficits, especially during the summer (Li et al., 2007; Nichols et al., 2009; Radu & Duval, 2018). The model also captured strong relationship to the stable variables like altitude (DEM) and sin_aspect (exposition), confirming that peatlands located in lowlands are more susceptible to negative effects of climate changes. Consequently, our spatial modelling illustrated the hydrological states of northern peatlands and their possible future conditions (Gallego-Sala et al., 2018; Loisel et al., 2021; Treat et al., 2022).

Lagged variables were important in our model. It is well known that ecological systems frequently show delayed responses to environmental change (Lira et al., 2019). In peatlands, this is plausible for testate amoebae because community composition can take time to adjust to new hydrological conditions. Experiments show detectable shifts within a few months after water-table manipulation, and transplantation studies show strong responses over 1 year (Koenig et al., 2017). In addition, reconstructions are commonly interpreted as reflecting mean annual moisture conditions, which can inherently smooth short-term variability and emphasize antecedent conditions. Seasonal variability in testate amoebae communities reported in field studies is consistent with the idea that the inferred hydrological signal integrates conditions over preceding months rather than a single date (Lamentowicz et al., 2013). Together, these points suggest that the strong performance of one-year lagged predictors in our models is ecologically plausible, but it also warrants cautious interpretation because the proxy and ecosystem may both incorporate earlier conditions.

We chose to evaluate our model using the area of applicability approach. Due to the limited number of samples, we initially anticipated that the model might not be applicable across the entire region. However, the AOA analysis enabled us to identify areas where field surveys are still insufficient. This insight provides valuable guidance for planning future ground-based pal-

aeoecological studies, ultimately improving prediction accuracy. The results underscore a significant lack of field data on WTD in high-latitude regions, particularly in the permafrost areas of Asia, with the most extensive data gaps occurring in the most remote and inaccessible locations. The lack of data from local monitoring of WTD changes in these regions, combined with the rapid changes occurring due to climate change, presents a significant challenge for accurately modeling the state of these ecosystems. Without reliable data, predicting how wetlands might shift, adapt, or contribute to broader climate feedback loops is difficult.

Consequences of peatland drying for fire trajectories

Previous studies have demonstrated that contrasting water table trends yield different greenhouse gas (GHG) emissions. Specifically, high and low water tables have been shown to increase GHG emissions, with flooded peatlands emitting more methane and dry ones more carbon dioxide (Jurasinski et al., 2016; Li et al., 2023; Tanneberger et al., 2021; Tiemeyer et al., 2020). Anthropogenic global warming deepens hydrological contrasts, leading to wetter peatlands in the areas where thawing of permafrost is observed (Hugelius et al., 2020; Schuur et al., 2022; Turetsky et al., 2020) and drying of subarctic, temperate and continental peatlands (Loisel et al., 2021; Swindles et al., 2019; Piilo et al. 2023). The progressing consequence of peatlands drying leads, for instance, to increased fire risk (Kettridge et al., 2015; Moore et al., 2021; Sim et al., 2023; Wilkinson et al., 2023). Our observations align with these findings, demonstrating a clear relationship between declining WTD and fire frequency. In regions where WTD has been consistently decreasing, we recorded a substantially higher incidence of fires than areas exhibiting rising WTD trends. The increased fire activity in drying peatlands can be attributed to several interrelated mechanisms. First, a lower WTD exposes deeper layers of peat to aerobic conditions, promoting decomposition and reducing the moisture retention capacity of the soil, which in turn enhances its flammability (Kettridge et al., 2015). Second, drying trends can lead to shifts in vegetation composition, with more fire-prone species colonizing degraded wetland areas, further exacerbating fire risk (Laine et al., 2021). Third, prolonged droughts, which are becoming more frequent due to climate change, interact with long-term WTD decline, creating conditions where fires ignite more easily and burn more intensely, often smoldering deep into the peat layers and releasing substantial amounts of stored carbon (Davies et al., 2013; Turetsky et al., 2015; Van Der Werf et al., 2017; Witze, 2020). Conversely, in regions where WTD trends indicate stable or wetting moisture levels, fire occurrences were significantly lower. This suggests that wetland conservation and hydrological restoration efforts could play a crucial role in mitigating fire risk in peat-dominated landscapes (Ellis et al., 2022). Protection of wetlands as water reservoirs and carbon sinks is especially important now when there is more evidence documenting replacement of dry *Sphagnum* habitats by sedge-dominated vegetation which is less effective in carbon sequestration, for example in the European sub-Arctic (Piilo et al., 2023). These findings emphasize the importance of continuous WTD monitoring as an integral component of fire risk assessment and peatland management strategies. Incorporating WTD levels into Arctic fire risk models is essential, as WTD directly influences peatland moisture and, consequently, fuel flammability. Lower WTD levels, often resulting from climate-induced drying trends, increase the susceptibility of peat to ignition and smoldering combustion, leading to more severe and prolonged fires (Gibson et al., 2018). Furthermore, hydrological trends in high-latitude peatlands

show the contemporary regime shifts (Zhang et al., 2022) into unstable states driven by global warming.

Conclusions

This study provides a comprehensive analysis of WTD trends in high-latitude peatlands across the permafrost areas of the Northern Hemisphere over the past two decades, offering critical insights into the hydrological responses of these sensitive ecosystems to global warming. By integrating peat records (WTD reconstructions based on testate amoebae), remote sensing data, and a diverse set of explanatory variables, we have developed a model that captures the divergent responses of peatlands to recent change, revealing both drying and wetting trends in different regions.

The key findings of this study highlight the role of climatic and environmental variables, such as the Climate Moisture Index, precipitation seasonality, and elevation, in driving WTD trends. These variables, combined with vegetation indices like the Enhanced Vegetation Index, provide a robust framework for modeling peatland hydrology. Our results demonstrate that drying trends are associated with increased wildfire occurrences. The application of machine learning techniques, particularly the Random Forest model, proved to be highly effective in predicting WTD trends, offering a balance between accuracy and interpretability.

While the model's accuracy is moderate, the results demonstrate the significant potential for modeling WTD in permafrost regions. Incorporating environmental variables related to topography, climate, and vegetation enhances our understanding of the processes driving WTD trends. However, the study also highlights the limitations of current models due to the scarcity of field data, particularly in remote and inaccessible regions of the Arctic. This underscores the need for expanded field campaigns to improve the accuracy and applicability of future models. In the future, it is essential to expand our research using additional training data and develop more nuanced models to analyze wetland trends in permafrost regions. Machine learning holds great promise for enhancing WTD modeling. Using more sophisticated techniques, such as neural networks, could improve model accuracy while offering deeper insights into wetland dynamics in a changing climate.

References

Andersen, D., Litvinchuk, S. N., Jang, H. J., Jiang, J., Koo, K. S., Maslova, I., Kim, D., Jang, Y., & Borzée, A. (2022). Incorporation of latitude-adjusted bioclimatic variables increases accuracy in species distribution models. *Ecological Modelling*, *469*, 109986. https://doi.org/10.1016/j.ecolmodel.2022.109986

Artz, R. R. E., Coyle, M., Donaldson-Selby, G., & Morrison, R. (2022). Net carbon dioxide emissions from an eroding Atlantic blanket bog. *Biogeochemistry*, *159*(2), 233–250. https://doi.org/10.1007/s10533-022-00923-x

Asmuß, T., Bechtold, M., & Tiemeyer, B. (2019). On the Potential of Sentinel-1 for High Resolution Monitoring of Water Table Dynamics in Grasslands on Organic Soils. *Remote Sensing*, *11*(14), Article 14. https://doi.org/10.3390/rs11141659

Austin, M. (2007). Species distribution models and ecological theory: A critical assessment and some possible new approaches. *Ecological Modelling*, *200*(1), 1–19. https://doi.org/10.1016/j.ecolmodel.2006.07.005

Beale, C. M., Lennon, J. J., Yearsley, J. M., Brewer, M. J., & Elston, D. A. (2010). Regression analysis of spatial data. *Ecology Letters*, *13*(2), 246–264. https://doi.org/10.1111/j.1461-0248.2009.01422.x

Bechtold, M., De Lannoy, G. J. M., Reichle, R. H., Roose, D., Balliston, N., Burdun, I., Devito, K., Kurbatova, J., Strack, M., & Zarov, E. A. (2020). Improved groundwater table and L-band brightness temperature estimates for Northern Hemisphere peatlands using new model physics and SMOS observations in a global data assimilation framework. *Remote Sensing of Environment*, *246*, 111805. https://doi.org/10.1016/j.rse.2020.111805

Bechtold, M., Schlaffer, S., Tiemeyer, B., & De Lannoy, G. (2018). Inferring Water Table Depth Dynamics from ENVISAT-ASAR C-Band Backscatter over a Range of Peatlands from Deeply-Drained to Natural Conditions. *Remote Sensing*, *10*(4), Article 4. https://doi.org/10.3390/rs10040536

Bechtold, M., Tiemeyer, B., Laggner, A., Leppelt, T., Frahm, E., & Belting, S. (2014). Large-scale regionalization of water table depth in peatlands optimized for greenhouse gas emission upscaling. *Hydrology and Earth System Sciences*, *18*(9), 3319–3339. https://doi.org/10.5194/hess-18-3319-2014

Beer, C., Runge, A., Grosse, G., Hugelius, G., & Knoblauch, C. (2023). Carbon dioxide release from retrogressive thaw slumps in Siberia. *Environmental Research Letters*, *18*(10), 104053. https://doi.org/10.1088/1748-9326/acfdbb

Belyea, L. R., & Baird, A. J. (2006). Beyond "the Limits to Peat Bog Growth": Cross-Scale Feedback in Peatland Development. *Ecological Monographs*, *76*(3), 299–322. https://doi.org/10.1890/0012-9615(2006)076[0299:BTLTPB]2.0.CO;2

Benscoter, B. W., & Wieder, R. K. (2003). Variability in organic matter lost by combustion in a boreal bog during the 2001 Chisholm fire. *Canadian Journal of Forest Research*, *33*(12), 2509–2513. https://doi.org/10.1139/x03-162

Blodau, C. (2002). Carbon cycling in peatlands □ A review of processes and controls. *Environmental Reviews*, *10*(2), 111–134. https://doi.org/10.1139/a02-004

Bourgeau-Chavez, L. L., Smith, K. B., Brunzell, S. M., Kasischke, E. S., Romanowicz, E. A., & Richardson, C. J. (2005). Remote monitoring of regional inundation patterns and hydroperiod in the Greater Everglades using Synthetic Aperture Radar. *Wetlands*, *25*(1), 176–191. https://doi.org/10.1672/0277-5212(2005)025[0176:RMORIP]2.0.CO;2

Bragazza, L. (2008). A climatic threshold triggers the die-off of peat mosses during an extreme heat wave. *Global Change Biology*, *14*(11), 2688–2695. https://doi.org/10.1111/j.1365-2486.2008.01699.x

Breiman, L. (2001). Random forests. *Machine Learning*, *45*(1), 5–32.

Brenning, A., Schwinn, M., Ruiz-Páez, A. P., & Muenchow, J. (2015). Landslide susceptibility near highways is increased by 1 order of magnitude in the Andes of southern Ecuador, Loja province. *Natural Hazards and Earth System Sciences*, *15*(1), 45–57. https://doi.org/10.5194/nhess-15-45-2015

Brun, P., Zimmermann, N. E., Hari, C., Pellissier, L., & Karger, D. N. (2022). Global climate-related predictors at kilometer resolution for the past and future. *Earth System Science Data*, *14*(12), 5573–5603.

Buchwal, A., Sullivan, P. F., Macias-Fauria, M., Post, E., Myers-Smith, I. H., Stroeve, J. C., Blok, D., Tape, K. D., Forbes, B. C., Ropars, P., Lévesque, E., Elberling, B., Angers-Blondin, S., Boyle, J. S., Boudreau, S., Boulanger-Lapointe, N., Gamm, C., Hallinger, M., Rachlewicz, G., … Welker, J. M. (2020). Divergence of Arctic shrub growth associated with sea ice decline. *Proceedings of the National Academy of Sciences*, *117*(52), 33334–33344. https://doi.org/10.1073/pnas.2013311117

Burdun, I., Bechtold, M., Aurela, M., De Lannoy, G., Desai, A. R., Humphreys, E., Kareksela, S., Komisarenko, V., Liimatainen, M., & Marttila, H. (2023). Hidden becomes clear: Optical remote sensing of vegetation reveals water table dynamics in northern peatlands. *Remote Sensing of Environment*, *296*, 113736.

Burdun, I., Bechtold, M., Sagris, V., Komisarenko, V., De Lannoy, G., & Mander, Ü. (2020). A Comparison of Three Trapezoid Models Using Optical and Thermal Satellite Imagery for Water Table Depth Monitoring in Estonian Bogs. *Remote Sensing*, *12*(12), Article 12. https://doi.org/10.3390/rs12121980

Burdun, I., Bechtold, M., Sagris, V., Lohila, A., Humphreys, E., Desai, A. R., Nilsson, M. B., De Lannoy, G., & Mander, Ü. (2020). Satellite Determination of Peatland Water Table Temporal Dynamics by Localizing Representative Pixels of A SWIR-Based Moisture Index. *Remote Sensing*, *12*(18), Article 18. https://doi.org/10.3390/rs12182936

Buttler, A., Bragazza, L., Laggoun-Défarge, F., Gogo, S., Toussaint, M.-L., Lamentowicz, M., Chojnicki, B. H., Słowiński, M., Słowińska, S., Zielińska, M., Reczuga, M., Barabach, J., Marcisz, K., Lamentowicz, Ł., Harenda, K., Lapshina, E., Gilbert, D., Schlaepfer, R., & Jassey, V. E. J. (2023). Ericoid shrub encroachment shifts aboveground–belowground linkages in three peatlands across Europe and Western Siberia. *Global Change Biology*, *29*(23), 6772–6793. https://doi.org/10.1111/gcb.16904

Canadell, J. G., Monteiro, P. M. S., Costa, M. H., Cunha, L. C. D., Cox, P. M., Eliseev, A. V., Henson, S., Ishii, M., Jaccard, S., Koven, C., Lohila, A., Patra, P. K., Piao, S., Syampungani, S., Zaehle, S., Zickfeld, K., Alexandrov, G. A., Bala, G., Bopp, L., … Lebehot, A. D. (2021). Global Carbon and other Biogeochemical Cycles and Feedbacks. In *IPCC AR6 WGI, Final Government Distribution* (p. chapter 5). https://hal.science/hal-03336145

Chadburn, S. E., Burke, E. J., Gallego-Sala, A. V., Smith, N. D., Bret-Harte, M. S., Charman, D. J., Drewer, J., Edgar, C. W., Euskirchen, E. S., Fortuniak, K., Gao, Y., Nakhavali, M., Pawlak, W., Schuur, E. A. G., & Westermann, S. (2022). A new approach to simulate peat accumulation, degradation and stability in a global land surface scheme (JULES vn5.8_accumulate_soil) for northern and temperate peatlands. *Geoscientific Model Development*, *15*(4), 1633–1657. https://doi.org/10.5194/gmd-15-1633-2022

Cohen, J. (1960). A coefficient of agreement for nominal scales. *Educational and Psychological Measurement*, *20*(1), 37–46.

Computing, Rf. (2013). R: A language and environment for statistical computing. *Vienna: R Core Team*.

Connolly, J., Holden, N. M., Connolly, J., Seaquist, J. W., & Ward, S. M. (2011). Detecting recent disturbance on Montane blanket bogs in the Wicklow Mountains, Ireland using the MODIS enhanced vegetation index. *International Journal of Remote Sensing*, *32*(9), 2377–2393. https://doi.org/10.1080/01431161003698310

Cruickshank, M. M., & Tomlinson, R. W. (1990). Peatland in Northern Ireland: Inventory and prospect. *Irish Geography*, *23*(1), 17–30.

Davies, D. K., Ilavajhala, S., Wong, M. M., & Justice, C. O. (2008). Fire information for resource management system: Archiving and distributing MODIS active fire data. *IEEE Transactions on Geoscience and Remote Sensing*, *47*(1), 72–79.

Davies, G. M., Gray, A., Rein, G., & Legg, C. J. (2013). Peat consumption and carbon loss due to smouldering wildfire in a temperate peatland. *Forest Ecology and Management*, *308*, 169–177. https://doi.org/10.1016/j.foreco.2013.07.051

Eberly, L. E. (2007). Multiple Linear Regression. In W. T. Ambrosius (Ed.), *Topics in Biostatistics* (pp. 165–187). Humana Press. https://doi.org/10.1007/978-1-59745-530-5_9

Ellis, T. M., Bowman, D. M. J. S., Jain, P., Flannigan, M. D., & Williamson, G. J. (2022). Global increase in wildfire risk due to climate-driven declines in fuel moisture. *Global Change Biology*, *28*(4), 1544–1559. https://doi.org/10.1111/gcb.16006

Evans, J. S., Murphy, M. A., Holden, Z. A., & Cushman, S. A. (2011). Modeling species distribution and change using random forest. In C. A. Drew, Y. F. Wiersma, & F. Huettmann (Eds.), *Predictive Species and Habitat Modeling in Landscape Ecology: Concepts and Applications* (pp. 139–159). Springer. https://doi.org/10.1007/978-1-4419-7390-0_8

Fischer, H., Meissner, K. J., Mix, A. C., Abram, N. J., Austermann, J., Brovkin, V., Capron, E., Colombaroli, D., Daniau, A.-L., Dyez, K. A., Felis, T., Finkelstein, S. A., Jaccard, S. L., McClymont, E. L., Rovere, A., Sutter, J., Wolff, E. W., Affolter, S., Bakker, P., … Zhou, L. (2018). Palaeoclimate constraints on the impact of 2 °C anthropogenic warming and beyond. *Nature Geoscience*, *11*(7), Article 7. https://doi.org/10.1038/s41561-018-0146-0

Gałka, M., Knorr, K.-H., Tobolski, K., Gallego-Sala, A., Kołaczek, P., Lamentowicz, M., Kajukało-Drygalska, K., & Marcisz, K. (2022). How far from a pristine state are the peatlands in the Białowieża Primeval Forest (CE Europe) – Palaeoecological insights on peatland and forest development from multiproxy studies. *Ecological Indicators*, *143*, 109421. https://doi.org/10.1016/j.ecolind.2022.109421

Gallego-Sala, A. V., Charman, D. J., Brewer, S., Page, S. E., Prentice, I. C., Friedlingstein, P., Moreton, S., Amesbury, M. J., Beilman, D. W., Björck, S., Blyakharchuk, T., Bochicchio, C., Booth, R. K., Bunbury, J., Camill, P., Carless, D., Chimner, R. A., Clifford, M., Cressey, E., … Zhao, Y. (2018). Latitudinal limits to the predicted increase of the peatland carbon sink with warming. *Nature Climate Change*, *8*(10), Article 10. https://doi.org/10.1038/s41558-018-0271-1

Gibson, C. M., Chasmer, L. E., Thompson, D. K., Quinton, W. L., Flannigan, M. D., & Olefeldt, D. (2018). Wildfire as a major driver of recent permafrost thaw in boreal peatlands. *Nature Communications*, *9*(1), Article 1. https://doi.org/10.1038/s41467-018-05457-1

Gorelick, N., Hancher, M., Dixon, M., Ilyushchenko, S., Thau, D., & Moore, R. (2017). Google Earth Engine: Planetary-scale geospatial analysis for everyone. *Remote Sensing of Environment, Big Remotely Sensed Data: Tools, Applications and Experiences*, *202*, 18–27. https://doi.org/10.1016/j.rse.2017.06.031

Guisan, A., Edwards, T. C., & Hastie, T. (2002). Generalized linear and generalized additive models in studies of species distributions: Setting the scene. *Ecological Modelling*, *157*(2), 89–100. https://doi.org/10.1016/S0304-3800(02)00204-1

Hamed, K. H., & Rao, A. R. (1998). A modified Mann-Kendall trend test for autocorrelated data. *Journal of Hydrology*, *204*(1–4), 182–196.

Harenda, K. M., Lamentowicz, M., Samson, M., & Chojnicki, B. H. (2018). The Role of Peatlands and Their Carbon Storage Function in the Context of Climate Change. In T. Zielinski, I. Sagan, & W. Surosz (Eds.), *Interdisciplinary Approaches for Sustainable Development Goals* (pp. 169–187). Springer International Publishing. https://doi.org/10.1007/978-3-319-71788-3_12

Hastie, T. J. (1992). Generalized Additive Models. In *Statistical Models in S*. Routledge.

Heinemeyer, A., & Swindles, G. T. (2018). Unraveling past impacts of climate change and land management on historic peatland development using proxy-based reconstruction, monitoring data and process modeling. *Global Change Biology*, *24*(9), 4131–4142. https://doi.org/10.1111/gcb.14298

Hijmans, R. J., Cameron, S. E., Parra, J. L., Jones, P. G., & Jarvis, A. (2005). Very high resolution interpolated climate surfaces for global land areas. *International Journal of Climatology: A Journal of the Royal Meteorological Society*, *25*(15), 1965–1978.

Hugelius, G., Loisel, J., Chadburn, S., Jackson, R. B., Jones, M., MacDonald, G., Marushchak, M., Olefeldt, D., Packalen, M., Siewert, M. B., Treat, C., Turetsky, M., Voigt, C., & Yu, Z. (2020). Large stocks of peatland carbon and nitrogen are vulnerable to permafrost thaw. *Proceedings of the National Academy of Sciences*, *117*(34), 20438–20446. https://doi.org/10.1073/pnas.1916387117

Jurasinski, G., Günther, A. B., Huth, V., Couwenberg, J., & Glatzel, S. (2016). Ecosystem services provided by paludiculture–greenhouse gas emissions. *Paludiculture—Productive Use of Wet Peatlands*.

Karpińska-Kołaczek, M., Kołaczek, P., Marcisz, K., Gałka, M., Kajukało-Drygalska, K., Mauquoy, D., & Lamentowicz, M. (2024). Kettle-hole peatlands as carbon hot spots: Unveiling controls of carbon accumulation rates during the last two millennia. *CATENA*, *237*, 107764. https://doi.org/10.1016/j.catena.2023.107764

Kettridge, N., Turetsky, M. R., Sherwood, J. H., Thompson, D. K., Miller, C. A., Benscoter, B. W., Flannigan, M. D., Wotton, B. M., & Waddington, J. M. (2015). Moderate drop in water table increases peatland vulnerability to post-fire regime shift. *Scientific Reports*, *5*(1), Article 1. https://doi.org/10.1038/srep08063

Kim, J.-W., Lu, Z., Gutenberg, L., & Zhu, Z. (2017). Characterizing hydrologic changes of the Great Dismal Swamp using SAR/InSAR. *Remote Sensing of Environment*, *198*, 187–202. https://doi.org/10.1016/j.rse.2017.06.009

Klinke, R., Kuechly, H., Frick, A., Förster, M., Schmidt, T., Holtgrave, A.-K., Kleinschmit, B., Spengler, D., & Neumann, C. (2018). Indicator-Based Soil Moisture Monitoring of Wetlands by Utilizing Sentinel and Landsat Remote Sensing Data. *PFG – Journal of Photogrammetry, Remote Sensing and Geoinformation Science*, *86*(2), 71–84. https://doi.org/10.1007/s41064-018-0044-5

Knoll, L., Breuer, L., & Bach, M. (2019). Large scale prediction of groundwater nitrate concentrations from spatial data using machine learning. *Science of the Total Environment*, *668*, 1317–1327.

Koenig, I., Schwendener, F., Mulot, M., & Mitchell, E. A. D. (2017). Response of Sphagnum Testate Amoebae to Drainage, Subsequent Re-wetting and Associated Changes in the Moss Carpet – Results from a Three Year Mesocosm Experiment. *Acta Protozoologica*, *2017*(Volume 56, Issue 3), 191–210.

Kursa, M. B., & Rudnicki, W. R. (2010). Feature selection with the Boruta package. *Journal of Statistical Software*, *36*, 1–13. https://doi.org/10.18637/jss.v036.i11

Laine, A. M., Korrensalo, A., Kokkonen, N. A. K., & Tuittila, E.-S. (2021). Impact of long-term water level drawdown on functional plant trait composition of northern peatlands. *Functional Ecology*, *35*(10), 2342–2357. https://doi.org/10.1111/1365-2435.13883

Lamentowicz, M., Bragazza, L., Buttler, A., Jassey, V. E. J., & Mitchell, E. A. D. (2013). Seasonal patterns of testate amoeba diversity, community structure and species–environment relationships in four *Sphagnum*-dominated peatlands along a 1300 m altitudinal gradient in Switzerland. *Soil Biology and Biochemistry*, *67*, 1–11. https://doi.org/10.1016/j.soilbio.2013.08.002

Lamentowicz, M., Gałka, M., Marcisz, K., Słowiński, M., Kajukało-Drygalska, K., Dayras, M. D., & Jassey, V. E. J. (2019). Unveiling tipping points in long-term ecological records from Sphagnum-dominated peatlands. *Biology Letters*, *15*(4), 20190043. https://doi.org/10.1098/rsbl.2019.0043

Leathwick, J. R., Elith, J., & Hastie, T. (2006). Comparative performance of generalized additive models and multivariate adaptive regression splines for statistical modelling of species distributions. *Ecological Modelling, Predicting Species Distributions*, *199*(2), 188–196. https://doi.org/10.1016/j.ecolmodel.2006.05.022

Lee, H., Calvin, K., Dasgupta, D., Krinner, G., Mukherji, A., Thorne, P., Trisos, C., Romero, J., Aldunce, P., & Barret, K. (2023). *IPCC, 2023: Climate Change 2023: Synthesis Report, Summary for Policymakers. Contribution of Working Groups I, II and III to the Sixth Assessment Report of the Intergovernmental Panel on Climate Change [Core Writing Team, H. Lee and J. Romero (eds.)]. IPCC, Geneva, Switzerland.* https://mural.maynoothuniversity.ie/17886/

Lees, K. J., Artz, R. R. E., Khomik, M., Clark, J. M., Ritson, J., Hancock, M. H., Cowie, N. R., & Quaife, T. (2020). Using Spectral Indices to Estimate Water Content and GPP in Sphagnum Moss and Other Peatland Vegetation. *IEEE Transactions on Geoscience and Remote Sensing*, *58*(7), 4547–4557. IEEE Transactions on Geoscience and Remote Sensing. https://doi.org/10.1109/TGRS.2019.2961479

Li, J., Jiang, M., Pei, J., Fang, C., Li, B., & Nie, M. (2023). Convergence of carbon sink magnitude and water table depth in global wetlands. *Ecology Letters*, *26*(5), 797–804. https://doi.org/10.1111/ele.14199

Li, W., Dickinson, R. E., Fu, R., Niu, G.-Y., Yang, Z.-L., & Canadell, J. G. (2007). Future precipitation changes and their implications for tropical peatlands. *Geophysical Research Letters*, *34*(1). https://doi.org/10.1029/2006GL028364

Lira, P. K., de Souza Leite, M., & Metzger, J. P. (2019). Temporal Lag in Ecological Responses to Landscape Change: Where Are We Now? *Current Landscape Ecology Reports*, *4*(3), 70–82. https://doi.org/10.1007/s40823-019-00040-w

Loisel, J., Gallego-Sala, A. V., Amesbury, M. J., Magnan, G., Anshari, G., Beilman, D. W., Benavides, J. C., Blewett, J., Camill, P., Charman, D. J., Chawchai, S., Hedgpeth, A., Kleinen, T., Korhola, A., Large, D., Mansilla, C. A., Müller, J., van Bellen, S., West, J. B., … Wu, J. (2021). Expert assessment of future vulnerability of the global peatland carbon sink. *Nature Climate Change*, *11*(1), Article 1. https://doi.org/10.1038/s41558-020-00944-0

Loisel, J., Gallego-Sala, A. V., & Yu, Z. (2012). Global-scale pattern of peatland *Sphagnum* growth driven by photosynthetically active radiation and growing season length. *Biogeosciences*, *9*(7), 2737–2746. https://doi.org/10.5194/bg-9-2737-2012

Lyons, S. K., & Willig, M. R. (2002). Species richness, latitude, and scale-sensitivity. *Ecology*, *83*(1), 47–58.

Magnan, G., Le Stum-Boivin, É., Garneau, M., Grondin, P., Fenton, N., & Bergeron, Y. (2019). Holocene vegetation dynamics and hydrological variability in forested peatlands of the Clay Belt, eastern Canada, reconstructed using a palaeoecological approach. *Boreas*, *48*(1), 131–146. https://doi.org/10.1111/bor.12345

Marcisz, K., Belka, Z., Dopieralska, J., Jakubowicz, M., Karpińska-Kołaczek, M., Kołaczek, P., Mauquoy, D., Słowiński, M., Zieliński, M., & Lamentowicz, M. (2023). Neodymium isotopes in peat reveal past local environmental disturbances. *Science of The Total Environment*, *871*, 161859. https://doi.org/10.1016/j.scitotenv.2023.161859

McHugh, M. L. (2013). The chi-square test of independence. *Biochemia Medica*, *23*(2), 143–149.

McLeod, A. I. (2005). Kendall rank correlation and Mann-Kendall trend test. *R Package Kendall*, *602*, 1–10.

Meyer, H., Milà, C., Ludwig, M., Linnenbrink, J., Schumacher, F., Otto, P., Reudenbach, C., Nauss, T., Pebesma, E., & Nowosad, J. (2025). *CAST: 'caret' Applications for Spatial-Temporal Models* (Version 1.0.3) [Computer software]. https://cran.r-project.org/web/packages/CAST/index.html

Meyer, H., & Pebesma, E. (2021). Predicting into unknown space? Estimating the area of applicability of spatial prediction models. *Methods in Ecology and Evolution*, *12*(9), 1620–1633.

Millard, K., & Richardson, M. (2018). Quantifying the relative contributions of vegetation and soil moisture conditions to polarimetric C-Band SAR response in a temperate peatland. *Remote Sensing of Environment*, *206*, 123–138. https://doi.org/10.1016/j.rse.2017.12.011

Moore, P. A., Didemus, B. D., Furukawa, A. K., & Waddington, J. M. (2021). Peat depth as a control on Sphagnum moisture stress during seasonal drought. *Hydrological Processes*, *35*(4), e14117. https://doi.org/10.1002/hyp.14117

Natali, S. M., Holdren, J. P., Rogers, B. M., Treharne, R., Duffy, P. B., Pomerance, R., & MacDonald, E. (2021). Permafrost carbon feedbacks threaten global climate goals. *Proceedings of the National Academy of Sciences*, *118*(21), e2100163118. https://doi.org/10.1073/pnas.2100163118

Nichols, J. E., Walcott, M., Bradley, R., Pilcher, J., & Huang, Y. (2009). Quantitative assessment of precipitation seasonality and summer surface wetness using ombrotrophic sediments from an Arctic Norwegian peatland. *Quaternary Research*, *72*(3), 443–451. https://doi.org/10.1016/j.yqres.2009.07.007

Olefeldt, D., Goswami, S., Grosse, G., Hayes, D. J., Hugelius, G., Kuhry, P., Sannel, B., Schuur, E. a. G., & Turetsky, M. R. (2016). Arctic Circumpolar Distribution and Soil Carbon of Thermokarst Landscapes, 2015. *ORNL DAAC*. https://doi.org/10.3334/ORNLDAAC/1332

Olefeldt, D., Hovemyr, M., Kuhn, M. A., Bastviken, D., Bohn, T. J., Connolly, J., Crill, P., Euskirchen, E. S., Finkelstein, S. A., Genet, H., Grosse, G., Harris, L. I., Heffernan, L., Helbig, M., Hugelius, G., Hutchins, R., Juutinen, S., Lara, M. J., Malhotra, A., … Watts, J. D. (2021). The Boreal–Arctic Wetland and Lake Dataset (BAWLD). *Earth System Science Data*, *13*(11), 5127–5149. https://doi.org/10.5194/essd-13-5127-2021

Pang, Y., Räsänen, A., Juselius-Rajamäki, T., Aurela, M., Juutinen, S., Väliranta, M., & Virtanen, T. (2023). Upscaling field-measured seasonal ground vegetation patterns with Sentinel-2 images in boreal ecosystems. *International Journal of Remote Sensing*, *44*(14), 4239–4261. https://doi.org/10.1080/01431161.2023.2234093

Piilo, S. R., Väliranta, M. M., Amesbury, M. J., Aquino-López, M. A., Charman, D. J., Gallego-Sala, A., Garneau, M., Koroleva, N., Kärppä, M., & Laine, A. M. (2023). Consistent centennial-scale change in European sub-Arctic peatland vegetation towards Sphagnum dominance–implications for carbon sink capacity. *Global Change Biology*.

Pörtner, H.-O., Roberts, D. C., Tignor, M. M. B., Poloczanska, E. S., Mintenbeck, K., Alegría, A., Craig, M., Langsdorf, S., Löschke, S., Möller, V., Okem, A., & Rama, B. (Eds.). (2022). *Climate Change 2022: Impacts, Adaptation and Vulnerability. Contribution of Working Group II to the Sixth Assessment Report of the Intergovernmental Panel on Climate Change.*

Qiu, C., Zhu, D., Ciais, P., Guenet, B., Peng, S., Krinner, G., Tootchi, A., Ducharne, A., & Hastie, A. (2019). Modelling northern peatland area and carbon dynamics since the Holocene with the ORCHIDEE-PEAT land surface model (SVN r5488). *Geoscientific Model Development*, *12*(7), 2961–2982. https://doi.org/10.5194/gmd-12-2961-2019

Radu, D. D., & Duval, T. P. (2018). Precipitation frequency alters peatland ecosystem structure and CO2 exchange: Contrasting effects on moss, sedge, and shrub communities. *Global Change Biology*, *24*(5), 2051–2065. https://doi.org/10.1111/gcb.14057

Räsänen, A., Tolvanen, A., & Kareksela, S. (2022a). Monitoring peatland water table depth with optical and radar satellite imagery. *International Journal of Applied Earth Observation and Geoinformation*, *112*, 102866. https://doi.org/10.1016/j.jag.2022.102866

Räsänen, A., Tolvanen, A., & Kareksela, S. (2022b). Monitoring peatland water table depth with optical and radar satellite imagery. *International Journal of Applied Earth Observation and Geoinformation*, *112*, 102866. https://doi.org/10.1016/j.jag.2022.102866

Rydin, H., Jeglum, J. K., & Bennett, K. D. (2013). *The Biology of Peatlands, 2e*. OUP Oxford.

Savtchenko, A., Ouzounov, D., Ahmad, S., Acker, J., Leptoukh, G., Koziana, J., & Nickless, D. (2004). Terra and Aqua MODIS products available from NASA GES DAAC. *Advances in Space Research, Trace Constituents in the Troposphere and Lower Stratosphere*, *34*(4), 710–714. https://doi.org/10.1016/j.asr.2004.03.012

Schubert, P., Eklundh, L., Lund, M., & Nilsson, M. (2010). Estimating northern peatland CO2 exchange from MODIS time series data. *Remote Sensing of Environment*, *114*(6), 1178–1189. https://doi.org/10.1016/j.rse.2010.01.005

Schuur, E. A. G., Abbott, B. W., Commane, R., Ernakovich, J., Euskirchen, E., Hugelius, G., Grosse, G., Jones, M., Koven, C., Leshyk, V., Lawrence, D., Loranty, M. M., Mauritz, M., Olefeldt, D., Natali, S., Rodenhizer, H., Salmon, V., Schädel, C., Strauss, J., … Turetsky, M. (2022). Permafrost and Climate Change: Carbon Cycle Feedbacks From the Warming Arctic. *Annual Review of Environment and Resources*, *47*(1), 343–371. https://doi.org/10.1146/annurev-environ-012220-011847

Setiawan, Y., Pawitan, H., Prasetyo, L. B., & Permatasari, P. A. (2017). Monitoring tropical peatland ecosystem in regional scale using multi-temporal MODIS data: Present possibilities and future challenges. *IOP Conference Series: Earth and Environmental Science*, *54*(1), 012052. https://doi.org/10.1088/1755-1315/54/1/012052

Sim, T. G., Swindles, G. T., Morris, P. J., Baird, A. J., Gallego-Sala, A. V., Wang, Y., Blaauw, M., Camill, P., Garneau, M., Hardiman, M., Loisel, J., Väliranta, M., Anderson, L., Apolinarska, K., Augustijns, F., Aunina, L., Beaulne, J., Bobek, P., Borken, W., … Zhang, H. (2023). Regional variability in peatland

burning at mid-to high-latitudes during the Holocene. *Quaternary Science Reviews*, *305*, 108020. https://doi.org/10.1016/j.quascirev.2023.108020

Słowińska, S., Słowiński, M., Marcisz, K., & Lamentowicz, M. (2022). Long-term microclimate study of a peatland in Central Europe to understand microrefugia. *International Journal of Biometeorology*, *66*(4), 817–832. https://doi.org/10.1007/s00484-022-02240-2

Stage, A. R. (1976). An expression for the effect of aspect, slope, and habitat type on tree growth. *Forest Science*, *22*(4), 457–460.

Stage, A. R., & Salas, C. (2007). Interactions of elevation, aspect, and slope in models of forest species composition and productivity. *Forest Science*, *53*(4), 486–492.

Swindles, G. T., Morris, P. J., Mullan, D. J., Payne, R. J., Roland, T. P., Amesbury, M. J., Lamentowicz, M., Turner, T. E., Gallego-Sala, A., Sim, T., Barr, I. D., Blaauw, M., Blundell, A., Chambers, F. M., Charman, D. J., Feurdean, A., Galloway, J. M., Gałka, M., Green, S. M., … Warner, B. (2019). Widespread drying of European peatlands in recent centuries. *Nature Geoscience*, *12*(11), Article 11. https://doi.org/10.1038/s41561-019-0462-z

Tanneberger, F., Moen, A., Barthelmes, A., Lewis, E., Miles, L., Sirin, A., Tegetmeyer, C., & Joosten, H. (2021). Mires in Europe—Regional Diversity, Condition and Protection. *Diversity*, *13*(8), Article 8. https://doi.org/10.3390/d13080381

Tiemeyer, B., Freibauer, A., Borraz, E. A., Augustin, J., Bechtold, M., Beetz, S., Beyer, C., Ebli, M., Eickenscheidt, T., Fiedler, S., Förster, C., Gensior, A., Giebels, M., Glatzel, S., Heinichen, J., Hoffmann, M., Höper, H., Jurasinski, G., Laggner, A., … Drösler, M. (2020). A new methodology for organic soils in national greenhouse gas inventories: Data synthesis, derivation and application. *Ecological Indicators*, *109*, 105838. https://doi.org/10.1016/j.ecolind.2019.105838

Toca, A., Villar-Salvador, P., Oliet, J. A., & Jacobs, D. F. (2020). Normalization criteria determine the interpretation of nitrogen effects on the root hydraulics of pine seedlings. *Tree Physiology*, *40*(10), 1381-1391,.

Torbick, N., Persson, A., Olefeldt, D., Frolking, S., Salas, W., Hagen, S., Crill, P., & Li, C. (2012). High Resolution Mapping of Peatland Hydroperiod at a High-Latitude Swedish Mire. *Remote Sensing*, *4*(7), Article 7. https://doi.org/10.3390/rs4071974

Treat, C. C., Jones, M. C., Alder, J., & Frolking, S. (2022). Hydrologic Controls on Peat Permafrost and Carbon Processes: New Insights From Past and Future Modeling. *Frontiers in Environmental Science*, *10*. https://www.frontiersin.org/articles/10.3389/fenvs.2022.892925

Tuittila, E.-S., Väliranta, M., Laine, J., & Korhola, A. (2007). Quantifying patterns and controls of mire vegetation succession in a southern boreal bog in Finland using partial ordinations. *Journal of Vegetation Science*, *18*(6), 891–902. https://doi.org/10.1111/j.1654-1103.2007.tb02605.x

Turetsky, M. R., Abbott, B. W., Jones, M. C., Anthony, K. W., Olefeldt, D., Schuur, E. A. G., Grosse, G., Kuhry, P., Hugelius, G., Koven, C., Lawrence, D. M., Gibson, C., Sannel, A. B. K., & McGuire, A. D. (2020). Carbon release through abrupt permafrost thaw. *Nature Geoscience*, *13*(2), Article 2. https://doi.org/10.1038/s41561-019-0526-0

Turetsky, M. R., Benscoter, B., Page, S., Rein, G., van der Werf, G. R., & Watts, A. (2015). Global vulnerability of peatlands to fire and carbon loss. *Nature Geoscience*, *8*(1), Article 1. https://doi.org/10.1038/ngeo2325

Van Der Werf, G. R., Randerson, J. T., Giglio, L., Van Leeuwen, T. T., Chen, Y., Rogers, B. M., Mu, M., Van Marle, M. J., Morton, D. C., & Collatz, G. J. (2017). Global fire emissions estimates during 1997–2016. *Earth System Science Data*, *9*(2), 697–720.

Vitt, D. H., Halsey, L. A., Bauer, I. E., & Campbell, C. (2000). Spatial and temporal trends in carbon storage of peatlands of continental western Canada through the Holocene. *Canadian Journal of Earth Sciences*, *37*(5), 683–693.

Wilkinson, S. L., Andersen, R., Moore, P. A., Davidson, S. J., Granath, G., & Waddington, J. M. (2023). Wildfire and degradation accelerate northern peatland carbon release. *Nature Climate Change*, *13*(5), Article 5. https://doi.org/10.1038/s41558-023-01657-w

Witze, A. (2020). The Arctic is burning like never before—And that's bad news for climate change. *Nature*, *585*(7825), 336–337. https://doi.org/10.1038/d41586-020-02568-y

Xie, X., Wu, T., Zhu, M., Jiang, G., Xu, Y., Wang, X., & Pu, L. (2021). Comparison of random forest and multiple linear regression models for estimation of soil extracellular enzyme activities in agricultural reclaimed coastal saline land. *Ecological Indicators*, *120*, 106925. https://doi.org/10.1016/j.ecolind.2020.106925

Yamazaki, D., Ikeshima, D., Neal, J. C., O'Loughlin, F., Sampson, C. C., Kanae, S., & Bates, P. D. (2017). *MERIT DEM: A new high-accuracy global digital elevation model and its merit to global hydrodynamic modeling*. *2017*, H12C-04.

Zhang, H., Väliranta, M., Swindles, G. T., Aquino-López, M. A., Mullan, D., Tan, N., Amesbury, M., Babeshko, K. V., Bao, K., Bobrov, A., Chernyshov, V., Davies, M. A., Diaconu, A.-C., Feurdean, A., Finkelstein, S. A., Garneau, M., Guo, Z., Jones, M. C., Kay, M., … Zhao, Y. (2022). Recent climate change has driven divergent hydrological shifts in high-latitude peatlands. *Nature Communications*, *13*(1), Article 1. https://doi.org/10.1038/s41467-022-32711-4

Zhang, H., Wu, P., Yin, A., Yang, X., Zhang, M., & Gao, C. (2017). Prediction of soil organic carbon in an intensively managed reclamation zone of eastern China: A comparison of multiple linear regressions and the random forest model. *Science of the Total Environment*, *592*, 704–713.

Zintzen, V., Anderson, M. J., Roberts, C. D., Harvey, E. S., & Stewart, A. L. (2017). Effects of latitude and depth on the beta diversity of New Zealand fish communities. *Scientific Reports*, *7*(1), 8081.

Zoltai, S. C., Morrissey, L. A., Livingston, G. P., & Groot, W. J. (1998). Effects of fires on carbon cycling in North American boreal peatlands. *Environmental Reviews*, *6*(1), 13–24. https://doi.org/10.1139/a98-002